

# **Crystal packing arrangement, chain conformation and physicochemical properties of gemfibrozil amine salts.**

Miren Ramirez<sup>†</sup>, Sarah E David<sup>†</sup>, Carl H Schwalbe<sup>†</sup>, Kofi Asare-Addo<sup>‡</sup>, Barbara R. Conway<sup>†</sup>, Peter Timmins \*<sup>§</sup>

<sup>†</sup>School of Life and Health Sciences, Aston University, Birmingham B4 7ET, UK; <sup>‡</sup>Department of Pharmacy, University of Huddersfield, Huddersfield HD1 3 DH, UK; <sup>§</sup>Drug Product Science and Technology, Bristol-Myers Squibb, Moreton, Merseyside CH46 1QW, UK.

**KEYWORDS:** Salt form; crystal packing; physicochemical properties; gemfibrozil; amines

## ABSTRACT

Salt formation is used to optimize pharmaceutical properties for carboxylic acid drugs but selection can often be empirical. An extended series of salts of the anti-hyperlipidaemia carboxylic acid drug gemfibrozil was prepared using related series of amine counterions to gain a molecular insight into the impact of crystal packing arrangements on their physicochemical properties. With only a few exceptions, the salts had similar crystal packing motifs. Although there was no discernible relationship between melting point of the salt form and the aqueous solubility of the salt across the whole dataset, there were trends within structurally-related series of salts relating increasing melting enthalpy with increasing molecular weight of the counter ion.

## INTRODUCTION

The crystal structure of an active pharmaceutical ingredient (API) will impact its physicochemical and mechanical properties, thus determining solubility, dissolution, stability, bioavailability and ultimately its successful application as a therapeutic agent. New chemical entities obtained by targeted drug design and combinatorial chemistry or high-throughput screening techniques often exhibit unfavourable qualities, most commonly low aqueous solubility and *in vivo* dissolution rate, while some show high hygroscopicity or other physical or chemical stability risks. Additional challenges in the development and manufacturing of potential APIs include undesirable physical and mechanical properties of the drug crystals and powder that can lead to difficulties during the processes of milling, filling, and compaction. Approaches that have been used to try to overcome these problems include salt formation<sup>1-5</sup>, crystallization solvent and conditions optimization, particle size reduction, or formation of solid dispersions, solid-lipid nanoparticle dispersions and complexation (e.g. with cyclodextrins)<sup>6,7</sup>.

Although salt formation is a widely-used strategy to improve solubility of ionisable drugs<sup>3,5,8,9</sup>, the choice of counterion for formation of the salt will potentially not only influence the physicochemical properties like solubility, but will likely also have an impact on the physical and mechanical properties of the drug. We have been particularly interested in the effects of amine counterions on the properties of carboxylic acid drugs, including crystal structure, solubility and other physicochemical properties and compaction behaviour<sup>10-13</sup>, as well as potential for impact on drug absorption through improved aqueous solubility. The favourable impact of the formation of diamine salts on the relative oral bioavailability of the anti-hyperlipidaemia carboxylic acid drug gemfibrozil has been demonstrated<sup>14</sup>. Understanding if and how salt form choices could be used to optimize pharmaceutical properties for carboxylic acid

drugs such as gemfibrozil would allow early selection and so speed clinical development for this class of compounds. We have therefore now extended the counterion range investigated for gemfibrozil (Fig. 1), beyond that we have previously studied<sup>11,12</sup> and also re-examined the previously investigated salt forms further, in order to gain additional understanding of molecular conformation and packing within the crystal and the influence on crystal properties.

## **EXPERIMENTAL SECTION**

### **Materials**

Gemfibrozil was pharmacopoeial grade (DiPharma, Italy) and *tert*-butylamine, tromethamine (tris), 2-amino-2-methylpropan-1-ol (AMP1), 2-amino-2-methylpropan-1,3-diol (AMP2) benzylamine, cyclopropylamine, cyclobutylamine, cyclohexylamine, octylamine, hexylamine, butylamine, triethanolamine, and adamantamine were analytical grade materials supplied by Sigma-Aldrich (Poole, UK). Acetonitrile and methanol were HPLC grade materials supplied by Fisher (Loughborough, UK).

### **Methods**

#### ***Salt preparation***

Crystalline salts were prepared by mixing equimolar amounts of drug and counterion dissolved in acetonitrile and recovering the precipitated salt by filtration under vacuum or by holding at -4°C until precipitate formed before filtration. Recovered salt precipitates were recrystallized from methanol. Salt formation was confirmed by nuclear magnetic resonance spectroscopy (NMR) and Fourier-transform infra-red spectroscopy (FTIR) and salt crystallinity examined by differential scanning calorimetry (DSC), looking for a sharp melting endotherm as indication of

production of a crystalline salt. <sup>1</sup>H NMR spectra were recorded on samples dissolved in deuterated chloroform on a Bruker AC 250 NMR (250 MHz) with a MAC Quadra 800 PC using WIN-NMR version 3.0 software. FTIR analysis of the drug or salt in KBr was carried out using a Unicam Mattson 3000 over 4000–400 cm<sup>-1</sup> with Galaxy software. DSC was performed using a calibrated Perkin Elmer PYRIS Diamond DSC. Each sample (3–5 mg) was accurately weighed and heated under nitrogen in vented pans at a scan rate of 10°C/min from 0°C to a temperature exceeding the melting point or a maximum of 250°C. FTIR, DSC and powder XRD data for the prepared salts are included in the supplementary information, Figs S1 – S5.

### ***Single crystal and powder X-ray diffractometry (XRD)***

Single-crystal X-ray diffraction data on the following five salts of gemfibrozil were collected at the National Crystallography Service, Southampton, UK: adamantylammonium (GAdam), benzylammonium (GBenz), cyclobutylammonium (GCbut), cyclohexylammonium (GChex) and triethanolammonium (GTea). Diffraction maxima, with MoK $\alpha$  ( $\lambda = 0.71073 \text{ \AA}$ ) radiation produced by a rotating anode generator, were collected with an area detector to a maximum  $\Theta$  approximately 27.5°. Multi-scan absorption corrections were applied with SADABS<sup>15</sup>. Structures were solved by direct methods with SHELXS<sup>16</sup>, revealing all non-hydrogen atoms. Non-hydrogen atom positions and anisotropic displacement parameters were refined with SHELXL2014/7<sup>17</sup>. Hydrogen atoms were assumed to ride on their attached atom, primary ammonium and methyl groups being allowed to rotate. Final discrepancy indices R(obs) reached 0.0851, 0.0498, 0.0603, 0.0442 and again 0.0442 for the five structures respectively. Crystallographic Information Files have been deposited with the Cambridge Crystallographic Data Centre.

### *Physicochemical properties*

Melting points and melting enthalpies were determined by DSC as outlined above. True densities were measured by helium pycnometry using a Gemini pycnometer (Micromeritics, Dunstable, UK) that was calibrated prior to use. To determine saturated solubility and solution pH, excess salt or free acid was added to double distilled water in a glass vial, the vial sealed and the contents stirred for 48 hours at ambient conditions (20 - 22°C) or in a water bath at 37°C. The supernatant solution in the vial was filtered through a 0.45µm PTFE syringe filter, pH measured using a pH meter with a glass electrode and the solution was then diluted for high-performance liquid chromatography analysis (HPLC). HPLC was undertaken using an Agilent 1100 series system (Agilent Technologies, Wokingham, UK) with a G1312A binary pump, a G1313A ALS autoinjector (injection volume 1µl), a G1316A COLCOM column section and a G1314A VWD variable wavelength detector set at 276 nm. Mobile phase was acetonitrile:water 65/35 v/v with 0.005% v/v phosphoric acid, delivered at 1 ml/min to a 15 cm x 4.6 mm C18 reverse phase column (ODS-2 Hypersil 5µm, ThermoScientific, Hemel Hempstead, UK).

## **RESULTS AND DISCUSSION**

Salt formation was confirmed by NMR and FTIR and all salts were confirmed as the expected 1:1 stoichiometry by NMR. No hydrates or solvates were identified as being formed based on thermal analysis data. Salts were found to be crystalline by DSC and powder XRD, although the butylamine, hexylamine, octylamine and cyclopropylamine salts were poorly crystalline as evidenced by their broad DSC melting endotherm and broad diffraction peaks on the powder XRD pattern. This limited the information we were able to develop for these compounds.

## Crystal structures of gemfibrozil amine salts

The crystallography of gemfibrozil free acid has been described previously<sup>18</sup> as have the crystal structures for the *tert*-butylamine, AMP1, AMP2 and tris salts, determined from powder XRD data, using the direct-space Genetic Algorithm technique and Rietveld refinement<sup>11</sup>.

Crystallographic data for the new adamantylamine, benzylamine, cyclobutylamine, cyclohexylamine, and triethanolamine salts are given in table 1. Refinement parameters were satisfactory, apart from the value of R(int) of 17.96 found for the adamantylammonium salt.

This was attributed to the difficulty in preparing large crystals of this salt and that the best crystal available used for crystal structure determination at approximately 0.2mm x 0.04mm x 0.01mm did result in a less than ideal signal to noise ratio. Repeating the refinement without the reflections above theta 25.25 degrees decreased the R(int) to 17.31%, a small improvement.

However, R factors for the agreement between observed and calculated data showed more improvement: wR2 dropped from 20.18% to 18.43% and the R factor for observed reflections went from 8.43% to 7.84%. Therefore, the determination of crystal structure was achieved for this salt, despite the rather small crystal size. Hydrogen bonding distances are provided in the supplementary information, Table S1.

For efficient packing within the crystal, gemfibrozil molecules must arrange to find interaction partners for the highly polar carboxylic acid or carboxylate group and the bulky nonpolar dimethylphenyl group. They can be kept well separated if the alkoxy chain adopts an all-*trans* conformation. The free acid has a monoclinic unit cell where the asymmetric unit is formed of two molecules with hydrogen bonding between the carboxylic acid groups. The geometric

parameters of the two molecules of the asymmetric unit are very similar. Essentially, the alkoxy chain adopts an extended conformation, the non-H atoms (excluding those of the carboxylic acids and the  $\alpha$ -methyl groups) lying more or less in a plane with the carboxylate group turned perpendicular to the plane of the side chain (Fig. 2a).

For the amine salts studied in this work, taking the cyclohexylammonium salt (Fig. 3) as representative, the torsion angles along the alkoxy side chain are defined as set out in table 2, where of the two carboxylate oxygen atoms, O1 is the one which defines a torsion angle with magnitude  $\leq 90^\circ$ . To provide more compact descriptors of the chain conformation the distances between the ether oxygen atom O3 and the carboxylate oxygen atoms O1 and O2 are tabulated (O...O distances, table 2). In the case of the free acid, all torsion angles are *trans* apart from TOR5 and TOR6, which are *gauche*. With only a few exceptions the salts show a similar pattern of torsion angles and distance of the ether oxygen O3 from the carboxylate oxygens O1 and O2. In the tris salt and both anions in the butane-1,4-diammonium salt<sup>14</sup> TOR3 is *gauche* but TOR5 is *trans*, providing a measure of compensation. Still, this change can enlarge the difference in ether to carboxylate O...O distances: in the case of the tris salt one O...O distance is the longest in the entire set while the other one is among the shortest. TOR3 in the *tert*-butylammonium salt is unlike any others.

To further explore these results for a wider range of structures with similar features, the conformation determined for the gemfibrozil anion in the cyclohexylammonium salt was employed as the query structure in torsion angle absolute values searches with the Cambridge Crystallographic Data Centre Mogul tool<sup>19</sup>. For the cyclohexylammonium salt, and hence all the

salts investigated except *tert*-butylammonium, tris and, as reported by others<sup>14</sup> butane-1,4-diammonium, the torsion angles TOR1, TOR2, TOR3 and TOR4 fall within the most populated ranges (*trans*), whilst TOR 5 is *gauche* - as are most of the comparison structures (Fig. 4). No preference is evident for TOR6. In the case of the tris and butane-1,4-diammonium salts, TOR3 is *gauche*, which is an alternate frequently populated range for this structure, but the angle for TOR3 in the case of the *tert*-butylammonium salt TOR3 is not within the frequently populated ranges. Hence the alkoxy chain in the *tert*-butylammonium salt of gemfibrozil is the most removed from a straight conformation (Fig. 2b).

For the unit cells, most of the salts, like the free acid, have one short cell axis in the range 6.2 – 6.5 Å, which may indicate the presence of a common crystal packing motif (Table 3). For the free acid, the short cell axis is larger at 7.36 Å, and this is also the case with the tris salt at 10.04 Å and also the triethanolammonium salt, where the short cell axis is 7.12 Å. Except for the cases of the triethanolammonium and tris salts (see later), the common short axis arises, as previously described for the *tert*-butylammonium, AMP1 and AMP2 salts, from chains of alternating gemfibrozil anions and amine cations linked by N-H $\cdots$ O (more correctly N<sup>+</sup>-H $\cdots$ O<sup>-</sup>, although in this paper, for simplicity, we have not indicated ionized forms in identifying specific discussed groups) hydrogen bonds<sup>11</sup>, with adjacent chain having cross-links in the form of N-H $\cdots$ O hydrogen bonds resulting in a ladder like structure. The “frame” of the ladder is made of hydrogen bonds backed up by the alternating hydrophobic and hydrophilic domains of cation and anion, and the “rungs” are the between chain hydrogen bonds. The two chains of the ladder and the adjacent pair of hydrogen bonds form a hydrogen bonded ring<sup>11</sup>. The primary aliphatic amine salts adamantylammonium, cyclobutylammonium and cyclohexylammonium salts have

ladders of  $R_4^3(10)$  rings (Fig. 5) as previously described for the *tert*-butylammonium salt<sup>11</sup>. In every case, the ammonium group donates one hydrogen bond to a carboxylate oxygen adjacent to it in its chain, another to  $\text{OCO}^-$  along the chain and a third to  $\text{OCO}^-$  along the “rung”, related by a twofold screw axis; the H...O contact distances for all the salts investigated are remarkably uniform within a range of 1.80 to 1.89 Å (Table S1). The benzylammonium salt instead has ladders of  $R_4^2(8)$  and  $R_4^4(12)$  rings (Fig. 6), which may be engendered by the need to accommodate the aromatic ring into the packing motif. Generated around inversion centres, the rings here also have H...O distances within the narrow ranges seen for the primary aliphatic amine salts (Table S1). For the alicyclic amines, the alkyl groups of the cation approach the gemfibrozil aliphatic chain, whereas the benzene ring of the cation in the benzylammonium salt is located edge-on in close proximity to the aromatic ring of gemfibrozil. This packing arrangement results in the ring structure and the more compact unit cell of the benzylammonium salt relative to the alicyclic ammonium salts. The two most commonly occurring hydrogen bonded supramolecular assemblies for chiral ammonium carboxylate salts in the Cambridge Structural Database are the ladders of  $R_4^3(10)$  rings for homochiral salts and ladders of  $R_4^2(8)$  and  $R_4^4(12)$  rings for heterochiral ammonium salts<sup>20</sup> the former also referred to as Type II chains and the latter as Type III chains<sup>21</sup>. In our salts, we see these commonly observed structures with achiral cations and anions and within the Cambridge Structural Database the Type II structure was seen equally with achiral and chiral ammonium ions (salts with achiral carboxylic acids). Additional hydrogen bonding or halogen bonding opportunities within the asymmetric unit due to the counterion can lead to the disruption of these most common ladder structures with impact on the physicochemical properties of the salts<sup>11, 20</sup>.

Table 3 also presents the volume per asymmetric unit and the Kitaigorodski packing index calculated with PLATON<sup>22</sup>. As expected, a bulkier cation generally leads to a larger volume of the asymmetric unit, but this trend can be modified by packing efficiency. Thus, the series of salts *tert*-butylamine, AMP1, AMP2 exhibits a *decrease* in asymmetric unit volume for each step, even though OH is replacing one H each time. The extra hydrogen bonding between chains significantly improves the packing efficiency. That the *tert*-butylammonium salt has the lowest packing index of the entire group may be related to distortion observed in TOR3.

As with the hydroxyl substituted derivatives of *tert*-butylamine (i.e. AMP1, AMP2 and tris)<sup>11</sup>, triethanolamine as a counterion offers opportunity for additional hydrogen bonding within the unit cell beyond the cross linking of the alternating cation and anion adjacent chains as seen in the aliphatic and alicyclic amine salts. The triethanolamine hydroxyl groups are hydrogen bonded to the carboxylate oxygens of gemfibrozil. In the protonated cation two of the H-N-C-C torsion angles are *gauche* (-38° and -41°) and one, H1-N1-C20-C21, is *trans* (-174°). Steric hindrance appears to block the approach of a gemfibrozil anion in N-H...OCO hydrogen bonding, which would be assisted by electrostatic interaction between the carboxylate oxygens and the protonated, positively charged nitrogen of the amine. Instead, the narrow window opened on one side by the positioning of the C20-C21-O6-H6 ethanol moiety allows cation-cation interaction around an inversion centre *via* N-H...O hydrogen bonding to a neighbouring hydroxyl group (Fig 7). Participation of every polar H atom in hydrogen bonds may help to explain the relatively high Kitaigorodski packing index of this structure (Table 3). A search of the Cambridge Structural Database for salts formed between carboxylic acids and triethanolamine revealed structure determinations of 14 different salts, comprising 17

independent ion pairs. In 12 of the cations all three H-N-C-C torsion angles are *gauche*, precluding any intermolecular N-H...O hydrogen bonding except with the blade-like cymantrenecarboxylate ion<sup>23</sup>. In the other 5 cations, as in the present structure, one of these torsion angles is *trans*. Of these 5 cations, one forms paired N-H...OH dimers, 3 form N-H...OH chains and one leaves the NH unused. Without a single exception, all N-C-C-O torsions are *gauche*. The hydrogen bonding structure adopted in the triethanolammonium salt prevents the formation of ladders as with the majority of the other salts we have investigated. Similarly, with its ability to form additional hydrogen bonding within the unit cell conferred by multiple hydroxyl group substitution on the amine counterion, the tris salt also does not adopt a ladder-like arrangement<sup>11</sup>.

The effect on crystal packing of systematically varying the length of the alkyl chain in diamine salts (of the form  $\text{H}_2\text{N}(\text{CH}_2)_n\text{NH}_2$ , where  $n = 3, 4$  or  $5$ ) of gemfibrozil has also been described previously<sup>14</sup>, where each ammonium group is associated with a gemfibrozil carboxylate anion, with some similar observations to the monoamine salts reported here. When  $n = 3$ , these groups form the familiar ladders of (10) rings along the *b* axis, connected to adjacent ladders via (18) rings, thereby creating a supramolecular sheet. Increasing  $n$  to 4 or 5 opens up the structure, allowing for inclusion of two water molecules into each asymmetric unit that participate in hydrogen bonding. Hydrates were not found in the case of the monoamine salts in this work.

Overall, salt formation led to an increase in density, the exceptions being the linear amine salts, and the greatest effect being seen with those salts that had additional opportunity for hydrogen

bonding within the unit cells. This increase in density correlated reasonably well with, unit cell volume and the packing index. As denser crystals might help with, for example, accommodating higher doses of drug into acceptable tablet sizes, forming a salt with greater density might be an advantage. Choosing a counterion that provides for increased hydrogen bonding might be of value in this situation, as salts where increased hydrogen bonding was possible in the unit cell tended to have the greater densities, although the resulting density advantage might be negated by the greater mass required in using the salt form to deliver a specific dose of the active free acid.

Although for a limited series of salts previously described in the literature<sup>8</sup>, by excluding two of the six data pairs, Gould was able to demonstrate a linear relationship between  $\log_{10}$  solubility and the reciprocal of the absolute melting temperature<sup>1</sup>. Others have also had success in identifying solubility-melting point relationships for drug salts<sup>24, 25, 26</sup>, yet there are examples where a correlation was not observed<sup>4, 27, 28</sup>. Examining our data for the solubility of amine salts of gemfibrozil (Table 4), we were unable to observe an overall trend or demonstrate a relationship between melting point of the salt form and the aqueous solubility of the salt. This is despite having an extended set of salts in the current set over our previous work. Solubility is a complex phenomenon dependent not only on the strength of lattice energy which must be overcome to enable the compound to go into solution and the ability of the molecule going into solution to engage in interactions with solvent molecules, but in the case of salts for the counterion to also similarly interact with the solvent and so facilitate salt solubility.

Within structurally-related counterion series of salts from the overall set there were however possible trends, with increased melting point with increasing molecular weight for the cyclic amine counterions cyclopropylamine, cyclobutylamine, cyclohexylamine yet a decrease in melting point with increasing molecular weight for the linear amine counterions butylamine, hexylamine, octylamine. However, in both these series there was a trend to increasing melting enthalpy with increasing molecular weight of the counterion. A possible explanation invokes the fact that at equilibrium the Gibbs free energy change  $\Delta G = \Delta H - T\Delta S$  must be zero. For the constrained cyclic amines there is a relatively small entropy increase upon breaking up the crystal. As  $\Delta H$  increases for the larger cations,  $T$  must increase so that  $T\Delta S$  can match it. For the linear amine counterions there is a larger positive  $\Delta S$  which becomes more pronounced for the longer chains, requiring a smaller  $T$  to offset  $\Delta H$ . This line of reasoning is supported by thermodynamic data<sup>29</sup> for the parent hydrocarbons of the amines. In the series propyl, butyl, hexyl, octyl the entropy of fusion in  $\text{J K}^{-1} \text{mol}^{-1}$  is 37.4, 45.2, 45.8, 49.0 for the cyclo-alkanes but spans the much wider range 41.3, 54.0, 73.2, 95.8 for the open-chain alkanes.

## CONCLUSION

A series of amine salts of the carboxylic acid drug, gemfibrozil, was prepared, crystal structures determined and physicochemical properties measured. Like the free acid, most of the salts, have one short cell axis, leading to a common crystal packing motif, with a ladder-like arrangement. A bulkier counterion generally leads to a larger volume of the asymmetric unit, but this trend was modified by packing efficiency. Counterions affording opportunities for additional hydrogen bonding within the unit cell, triethanolamine and tris, hamper formation of this common motif.

Based on the results in this study, it can be concluded that, although salt formation increases solubility for all the counterions studied, it is not possible to make wide-ranging predictions of solubility based on the properties of the counterion used, although there are trends within structurally-related series. A thorough examination of the crystal arrangements within the different series provides a rational explanation for the different physicochemical properties determined.

## ASSOCIATED CONTENT

### **Supporting Information**

FTIR, DSC and powder XRD data for the prepared salts are included in the supplementary information, Figs. S1 – S5. A table of hydrogen bond distances and bond angles is also provided (Table S1).

### **Accession Codes**

The crystallographic data for the gemfibrozil salts reported in this paper that have not previously been previously described has been added to The Cambridge Structural Database as follows:

adamantylammonium, CCDC 1535728; benzylammonium, CCDC 1535729;

cyclobutylammonium, CCDC 1535730; cyclohexylammonium, CCDC 1535731;

triethanolammonium, CCDC 1535732. These data can be accessed via

[www.ccdc.cam.ac.uk/data\\_request/cif](http://www.ccdc.cam.ac.uk/data_request/cif), or by email to [data\\_request@ccdc.cam.ac.uk](mailto:data_request@ccdc.cam.ac.uk), or by

contacting The Cambridge Crystallographic Data Centre, 12 Union Road, Cambridge CB2 1 EZ, UK; fax +44 1223 336033.

## AUTHOR INFORMATION

### **Corresponding Author**

\*(PT) petertimmins918@btinternet.com

### **Present Addresses**

† (MR) Santa Maria de la Providencia School, 20600 Eibar, Spain

† (SED) Novartis AG, Lichtstrasse 35, Basel 40566, Switzerland

† (CHS) Cambridge Crystallographic Data Centre, 12 Union Road, Cambridge CB2 1EZ, UK

† (BRC) Department of Pharmacy University of Huddersfield, Huddersfield HD1 3DH, UK

§ (PT) Department of Pharmacy, University of Huddersfield, Huddersfield HD1 3DH, UK

## ACKNOWLEDGMENT

We thank P. N. Horton, R. Stephenson and G. J. Tizzard of the National Crystallography Service, Southampton, for data collection. This work constitutes part of the PhD theses submitted by Sarah David and Miren Ramirez and the authors thank Bristol-Myers Squibb for financial support for Sarah David and Miren Ramirez.

## REFERENCES

1. Gould, P. *Int. J. Pharm.* **1986**, *33*, 201 – 217.
2. Morris, K.R.; Fakes, M.G.; Thakur, A.B.; Newman, A.W.; Singh, A.K.; Venit, J.J.; Spagnuolo, C.J.; Serajuddin, A.T.M. *Int. J. Pharm.* **1994**, *105*, 209 – 217, ()
3. Stahl, P.H.; Wermuth, G. *Handbook of pharmaceutical salts: properties, selection and use*, Wiley-VCH, (2002).
4. Black, S.N.; Collier, E.A.; Davey, R.J.; Roberts, R.J. *J. Pharm. Sci.* **2007**, *96*, 1053 – 1068.
5. Serajuddin, A.T.M. *Adv. Drug Deliv. Rev.* **2007** *59*, 603 – 616.
6. York, P. *Drug Dev. Ind. Pharm.* **1992**, *18*, 677 – 721, ()
7. Williams, H.D.; Trevaskis, N.L.; Charman, S.A.; Shanker, R.M.; Charman, W.N.; Pouton, C.W.; Porter, C.J.H. *Pharmacol. Rev.* **2013**, *65*, 315 – 499.
8. Agharkar, S.; Lindenbaum, S.; Higuchi, T. *J. Pharm. Sci.* **1976**, *65*, 747 – 749.
9. Jones, P.H.; Rowley, E.K.; Weiss, A.L.; Bishop, D.L.; Chun, A.H.C. *J. Pharm. Sci.* **1969**, *58*, 337 – 339.
10. David, S.E.; Timmins, P.; Irwin, W.J.; Conway, B.R. *The effect of added counterions on the mechanical properties of a poorly compressible drug, gemfibrozil*; presented at Pharm Sci Fair, Nice (2005).

11. Cheung, E.Y.; David, S.E.; Harris, K.D.M.; Conway, B.R.; Timmins, P. *J. Solid State Chem.* **2007**, *180*, 1068 – 1075.
12. David, S.E.; Ramirez, M.; Timmins, P.; Conway, B.R. *J. Pharm. Pharmac.* **2010**, *62*, 1519 – 1525.
13. David, S.E.; Timmins, P.; Conway, B.R. *Drug Dev. Ind. Pharm.* **2012**, *38*, 93 – 103.
14. Yang, Q; Tianming, R.; Yang, S.; Li, X.; Chi, Y.; Yang, Y.; Gu, G.; Hu, C. *Cryst. Growth Des.* **2016**, *16*, 6060 - 6068.
15. Sheldrick, G.M. *SABDABS*, University of Göttingen, Göttingen, Germany (1996).
16. Sheldrick, G.M. *Acta Crystallogr. Sect. A*, **2008**, *64*, 112 -122
17. Sheldrick, G.M. *Acta Cryst.* **2015**, *C71*, 3 - 8
18. Bruni, B.; Coran, S.; Di Vaira, S.M.; Giannellini, V. *Acta Cryst.* **2005**, *E61*, o1989 – o1991.
19. Bruno, I.J.; Cole, J.C.; Kessler, M.; Luo, J.; Motherwell, W.D.S.; Purkis, L.H.; Smith, B.R.; Taylor, R.; Cooper, R.I.; Harris, S.E.; Orpen, A.G. *J. Chem. Inf. Comput. Sci.* **2004**, *44*, 2133 - 2144.
20. Lemmerer, A.; Bourne, S.A.; Fernandes, M.A. *CrystEngComm.* **2008**, *10*, 1750 - 1757.  
  
Kinbara, K.; Kai, A.; Maekawa, Y.; Hashimoto, Y.; Naruse, S.; Hasegawa, M.; Saigo, K. *J.Chem.Soc. Perkin Trans.* **1999**, *2*, 247 - 253.
21. Spek, A.L. *J. Appl. Crystallogr.* **2003**, *36*, 7 - 13

22. Ilyukhin, A.B.; Koroteev, P.S.; Kiskin, M.A.; Dobrokhotova, Z.V.; Novotortsev, V.M. *J. Mol. Struct.* **2013**, *1033*, 187-199
23. Anderson, B.D.; Conradi, R.A. *J. Pharm. Sci.* **1985**, *74*, 815 – 820.
24. Thomas, E.; Rubino, J. *Int. J. Pharm.* **1996**, *130*, 179 – 183.
25. K.M. O'Connor, O.I. Corrigan, *Int. J. Pharm.* 2001, *226*, 163 – 179.
26. Gu, L.; Strickley, R.G. *Pharm Res.* **1987**, *4*, 255 – 257.
27. Fini, A.; Cavallari, C.; Ospitali, F. *Pharmaceutics*, **2010**, *2*, 136 – 158.
28. Domalski, E.S.; Evans, W.H.; Hearing, E.D. *J. Phys. Chem. Ref. Data*, **1984**, *13*, Suppl. 1.

**Table 1.** Crystallographic data for gemfibrozil amine salts

	<b>GAdam</b>	<b>GBenz</b>	<b>GCbut</b>	<b>GChex</b>	<b>GTea</b>
Empirical formula	C <sub>25</sub> H <sub>39</sub> NO <sub>3</sub>	C <sub>22</sub> H <sub>31</sub> NO <sub>3</sub>	C <sub>19</sub> H <sub>31</sub> NO <sub>3</sub>	C <sub>21</sub> H <sub>35</sub> NO <sub>3</sub>	C <sub>21</sub> H <sub>37</sub> NO <sub>6</sub>
Molecular weight	401.57	357.48	321.45	349.50	399.51
Temperature (K)	120	120	120	120	120
Wavelength (Å)	0.71073	0.71073	0.71073	0.71073	0.71073
Crystal system	Orthorhombic	Triclinic	Orthorhombic	Monoclinic	Monoclinic
Space group	<i>P</i> 2 <sub>1</sub> 2 <sub>1</sub> 2 <sub>1</sub>	<i>P</i> -1	<i>P</i> 2 <sub>1</sub> 2 <sub>1</sub> 2 <sub>1</sub>	<i>P</i> 2 <sub>1</sub> / <i>n</i>	<i>P</i> 2 <sub>1</sub> / <i>c</i>
<i>a</i> (Å)	6.5081(4)	6.1974(3)	6.1793(4)	9.5074(6)	18.0782 (3)
<i>b</i> (Å)	10.5426(7)	12.7063(7)	9.3558(5)	6.5298(3)	7.10680(10)
<i>c</i> (Å)	34.282(3)	12.9893(6)	33.270(2)	32.936(2)	18.5776(4)
$\alpha$ (°)	90	91.917(2)	90	90	90
$\beta$ (°)	90	95.769(3)	90	90.340(2)	112.3770(10)
$\gamma$ (°)	90	95.241(3)	90	90	90
<i>V</i> (Å <sup>3</sup> )	2352.2(3)	1012.48(9)	1923.4(2)	2044.7(2)	2207.08(7)
<i>Z</i>	4	2	4	4	4
$\rho$ (g cm <sup>-3</sup> )	1.134	1.173	1.110	1.135	1.202
$\mu$ (mm <sup>-1</sup> )	0.073	0.077	0.074	0.074	0.087
<i>F</i> (000)	880	388	704	768	872
<i>Goof</i>	0.990	1.038	1.044	1.062	1.019
Reflections/data/parameters	21489/5111/268	21229/4631/244	11402/4300/213	12577/4117/232	36961/5060/261
<i>R</i> <sub>int</sub>	0.1796	0.0594	0.0472	0.0361	0.0577
Final <i>R</i> indices ( <i>I</i> > 2σ( <i>I</i> ))	<i>R</i> 1 = 0.0851 w <i>R</i> 2 = 0.1430	<i>R</i> 1 = 0.0500 w <i>R</i> 2 = 0.1125	<i>R</i> 1 = 0.0603 w <i>R</i> 2 = 0.1308	<i>R</i> 1 = 0.0442 w <i>R</i> 2 = 0.1051	<i>R</i> 1 = 0.0420 w <i>R</i> 2 = 0.1039
Final <i>R</i> indices (all data)	<i>R</i> 1 = 0.2453 w <i>R</i> 2 = 0.2018	<i>R</i> 1 = 0.0790 w <i>R</i> 2 = 0.1258	<i>R</i> 1 = 0.0754 w <i>R</i> 2 = 0.1410	<i>R</i> 1 = 0.0615 w <i>R</i> 2 = 0.1156	<i>R</i> 1 = 0.0609 w <i>R</i> 2 = 0.1139

**Table 2.** Alkoxy side chain torsion angles (to nearest degree) \* for gemfibrozil free acid and amine salts

Gemfibrozil salt	TOR1	TOR2	TOR3	TOR4	TOR5	TOR6	ShortOO <sup>a</sup>	LongOO <sup>a</sup>
Free acid a	179	-177	-178	-174	-55 <sup>b</sup>	-68 <sup>b</sup>	5.47	5.61
Free acid b	179	180	-177	-176	-53 <sup>b</sup>	-60 <sup>b</sup>	5.42	5.69
<i>tert</i> -butylammonium	-140 <sup>b</sup>	-172	-111 <sup>b</sup>	-158	-44 <sup>b</sup>	93 <sup>b</sup>	5.31	5.49
AMP1 salt	164	-163	-156	170	29 <sup>b</sup>	53 <sup>b</sup>	5.17	5.84
AMP2 salt	166	-166	180	166	-60 <sup>b</sup>	-68 <sup>b</sup>	5.44	5.51
tris salt	-171	-179	-64 <sup>b</sup>	-174	-171	51 <sup>b</sup>	5.22	6.32
adamantylammonium	177	177	-173	-167	59 <sup>b</sup>	62 <sup>b</sup>	5.42	5.53
benzylammonium	176	-175	-168	-178	67 <sup>b</sup>	70 <sup>b</sup>	5.55	5.87
cyclobutylammonium	-175	168	174	169	49 <sup>b</sup>	54 <sup>b</sup>	5.18	5.59
cyclohexylammonium	-179	-178	-177	-169	-50 <sup>b</sup>	-58 <sup>b</sup>	5.39	5.63
triethanolammonium	-177	-171	-171	-165	-64 <sup>b</sup>	48 <sup>b</sup>	5.32	5.89

\*The definition of torsion angles follows the numbering scheme illustrated in Figure 3 for the cyclohexylammonium salt, where the carboxylate oxygen atoms O1 and O2 are numbered such that the magnitude of TOR6 is  $\leq 90^\circ$  or the smaller of the two possible values: TOR1 = C13-C8-O3-C7, TOR2 = C8-O3-C7-C6, TOR3 = O3-C7-C6-C5, TOR4 = C7-C6-C5-C2, TOR5 = C6-C5-C2-C1, TOR6 = C5-C2-C1-O1.

<sup>a</sup> = distances from O3 to O2/O1

<sup>b</sup> = Torsion angle outside the antiperiplanar range.

**Table 3.** Unit cell dimensions for gemfibrozil free acid and amine salts\*

Gemfibrozil salt	<i>a</i> (Å)	<i>b</i> (Å)	<i>c</i> (Å)	Cell Volume (Å <sup>3</sup> )	Asymmetric unit volume (Å <sup>3</sup> )	Packing Index (%)
Free acid	14.86	7.36	27.95	3053.1	382	62.0
<i>tert</i> -butylammonium	6.45	9.68	33.10	2066.1	517	61.8
AMP1 salt	26.88	6.37	23.92	4092.8	512	64.4
AMP2 salt	27.08	6.32	22.89	3918.0	490	68.9
tris salt	18.50	10.04	11.00	2014.9	506	67.0
adamantylammonium	6.51	10.54	34.28	2352.2	588	65.5
benzylammonium	6.20	12.71	12.99	1012.5	506	67.9
cyclobutylammonium	6.18	9.36	33.27	1923.4	481	65.2
cyclohexylammonium	9.51	6.53	32.94	2044.7	511	67.4
triethanolammonium	18.08	7.11	18.58	2207.1	552	67.9

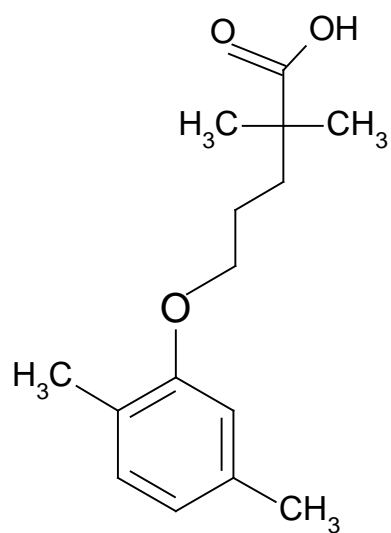
\*Hydrogen bond information is provided as part of the supplementary information

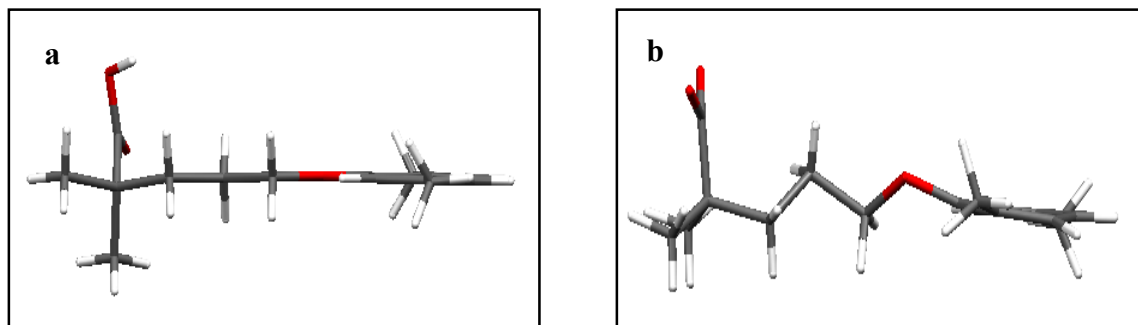
**Table 4.** Physicochemical properties of gemfibrozil salts

Salt counterion	Density (g/cm <sup>3</sup> )	Melting point (°C)	Enthalpy of fusion (kJ/mole)	Aqueous solubility (mg/ml)		pH of solution (ambient temperature samples)
				20 - 22°C	37°C	
none	1.09	61.2	25.2	0.039	0.002	4.62
butylamine	1.07	71.3	9.4	35.9	<sup>s</sup>	8.70
hexylamine	0.98	68.6	11.7	3.73	<sup>s</sup>	7.80
octylamine	0.75	49.2	19.5	0.88	<sup>s</sup>	7.50
benzylamine	1.13	94.3	28.0	1.73	4.41	8.32
cyclohexylamine	1.14	134.2	30.4	3.20	2.36	7.37
<i>t</i> -butylamine	1.04	133.6	30.4	11.03	7.82	7.78
AMP1	1.10	107.4	31.5	16.62	*	7.89
AMP2	1.21	119.7	44.3	25.2	13.16	8.10
tris	1.22	122.1	47.4	6.97	28.50	7.60
cyclopropylamine	1.14	85.0	7.5	4.28	14.24	8.02
cyclobutylamine	1.12	105.0	20.8	4.28	20.39	8.06
1-adamantylamine	1.14	192.9	37.7	0.19	0.59	5.96
triethanolamine	1.16	97.1	44.1	16.64	7.87	7.71

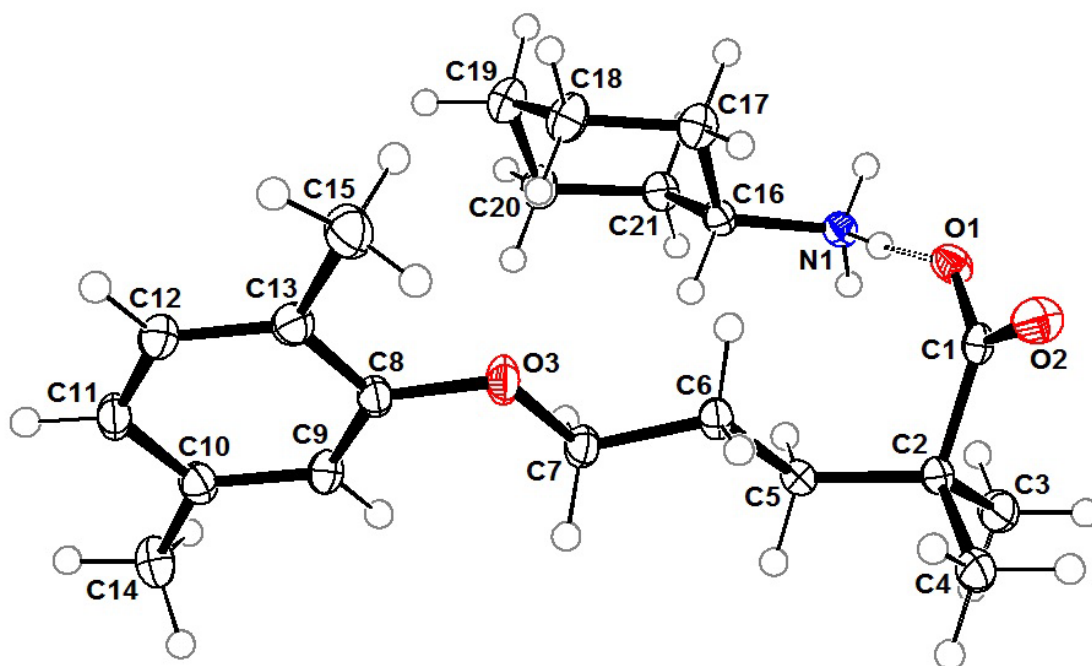
\* > 300 mg/mL saturation not achieved with limited amount of material available. <sup>s</sup>forms oily dispersion on shaking excess of salt with water at 37°C which solidifies and precipitates out on cooling to yield original salt form.

Figure 1. Structure of gemfibrozil





**Figure 2.** (a) Gemfibrozil, free acid form, in the unit cell viewed from the plane of the aromatic ring, (b) Gemfibrozil, from its *tert*-butylammonium salt form, in the unit cell viewed from the plane of the aromatic ring to show effect of counterion on side chain conformation.



**Figure 3.** Gemfibrozil cyclohexylammonium salt

**Figure 4.** Frequency plots based on data in the Cambridge Structural Database for torsion angles examined in gemfibrozil and its amine salts, determined using CSSD Mogul. Query values marked are for cyclohexylammonium salt.

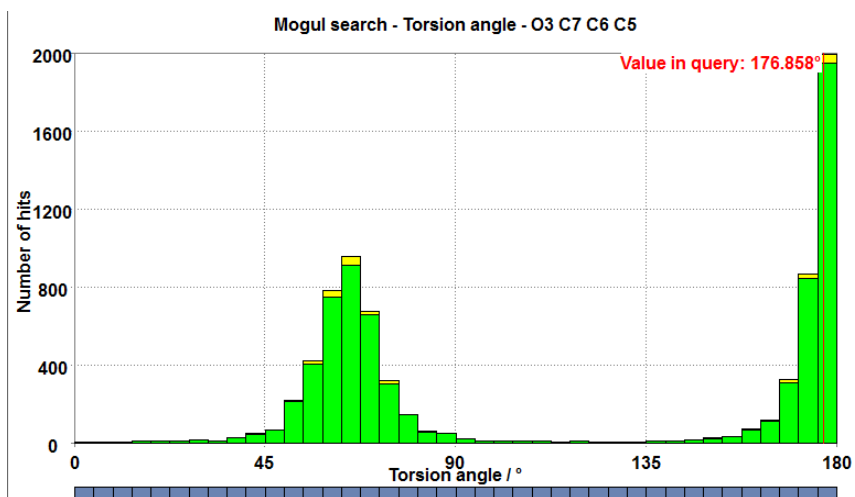
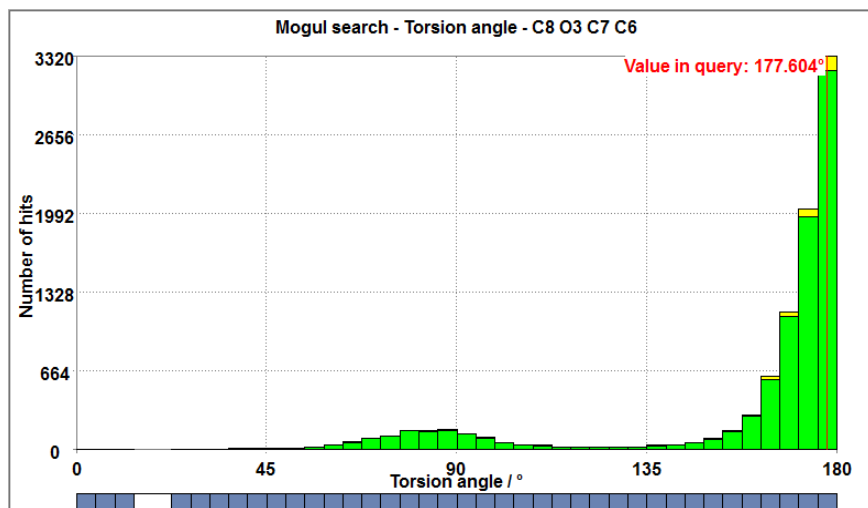
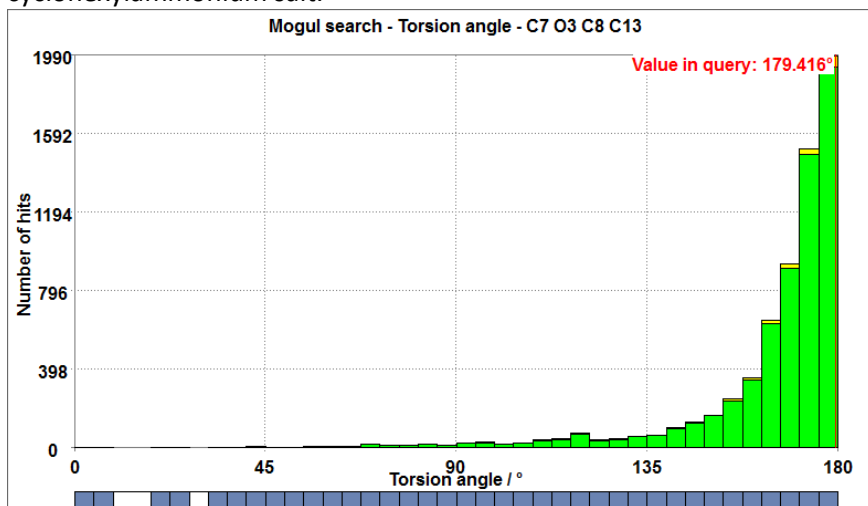
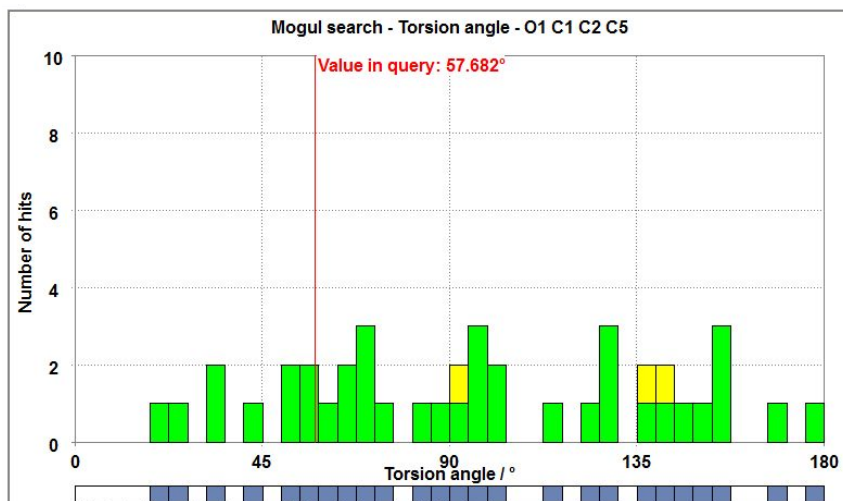
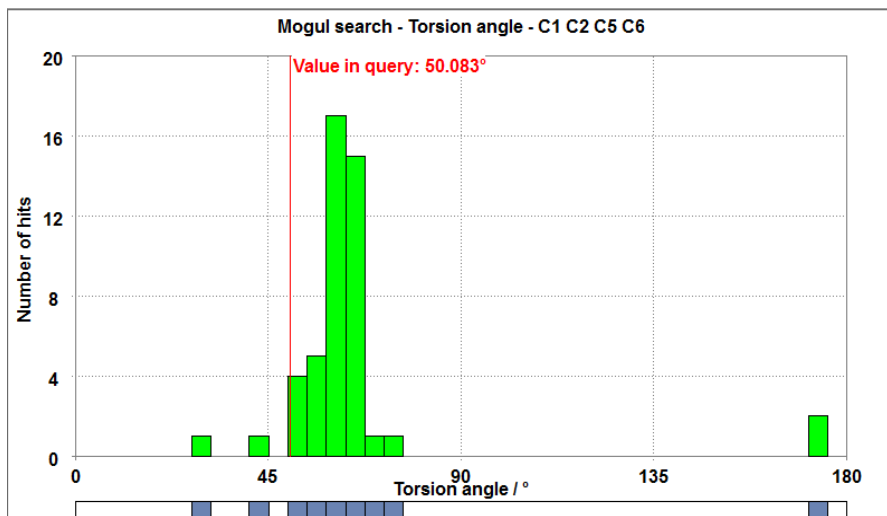
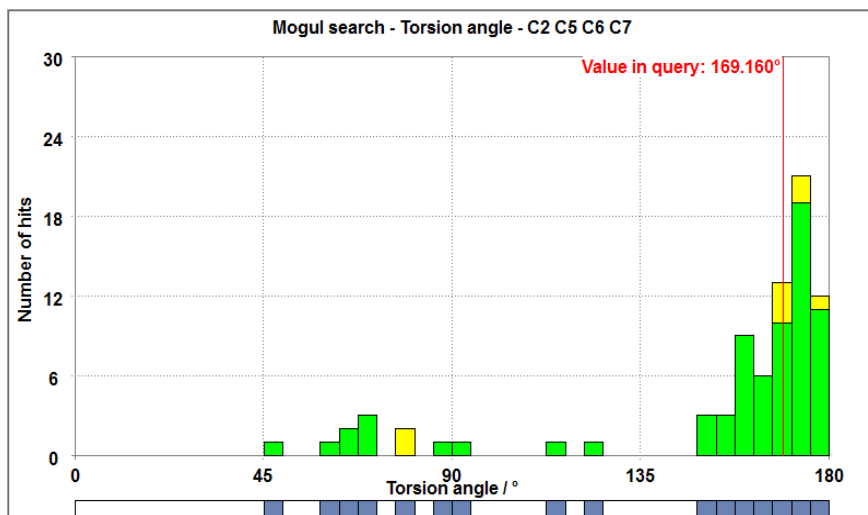
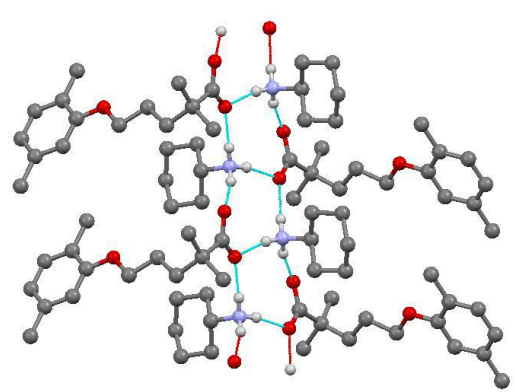
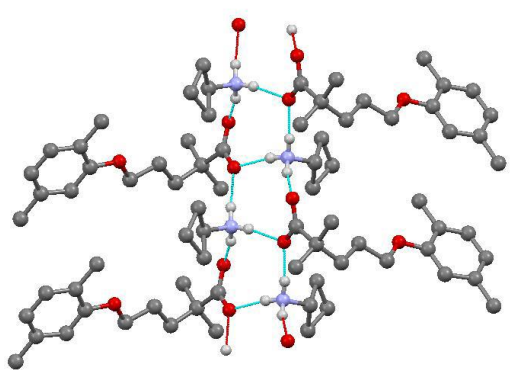
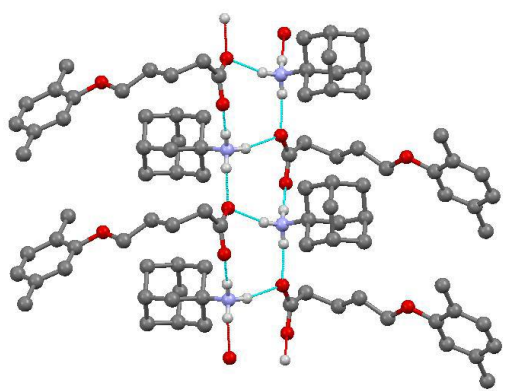
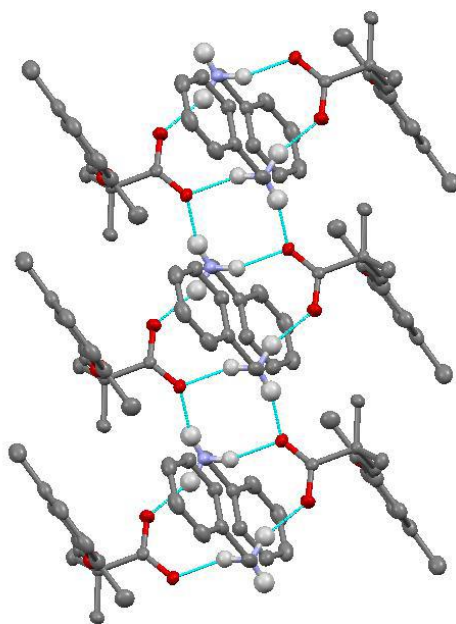


Figure 4. (continued)





**Figure 5.** Crystal structure for gemfibrozil adamantylammonium salt (top), gemfibrozil cyclobutylammonium salt (centre) and gemfibrozil cyclohexylammonium salt (bottom), with hydrogen bonds indicated by blue connectors to show the ladders of  $R_4^3(10)$  rings supramolecular assembly.



**Figure 6.** Crystal structure of gemfibrozil benzylammonium salt, with hydrogen bonds indicated by blue connectors to show the ladders of  $R_4^2(8)$  and  $R_4^1(12)$  rings supramolecular assembly.

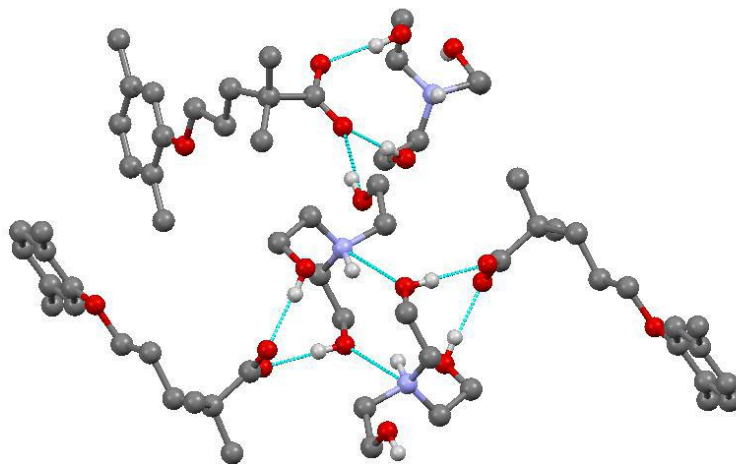


**Figure 7.** Crystal structure of gemfibrozil triethanolammonium salt, with hydrogen bonds indicated by blue connectors showing this salt does not exhibit the ladders of rings supramolecular assembly seen in many of the other amine salts.